Transportation Research Interdisciplinary Perspectives 24 (2024) 101079

Contents lists available at ScienceDirect

Transportation Research Interdisciplinary Perspectives

journal homepage: www.sciencedirect.com/journal/transportation-research-interdisciplinary-perspectives

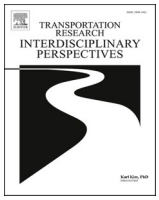

Optimizing the location and configuration of disaster resilience hubs under transportation and electric power network failures

Daniel Rodriguez-Roman [a,*], Hector J. Carlo [b], Joshua Sperling [c], Andrew Duvall [c], Rubén E. Leoncio-Cabán [d], Carla López del Puerto [a]

[a] Department of Civil Engineering and Surveying, University of Puerto Rico - Mayagüez, Mayagüez 00681, Puerto Rico
[b] Department of Industrial Engineering, University of Puerto Rico - Mayagüez, Mayagüez 00681, Puerto Rico
[c] National Renewable Energy Laboratory, 15013 Denver W Pkwy, Golden, CO 80401, United States
[d] Department of Electrical Engineering, University of Puerto Rico - Mayagüez, Mayagüez, PR 00681, Puerto Rico

ARTICLE INFO

Keywords:
Facility location
Energy
Transportation networks
Disasters
Resilience
Accessibility

ABSTRACT

Natural disasters often result in failures of transportation network components and blackouts that imperil the wellbeing of vulnerable populations. In response to these events, resilience hubs have been proposed as a pre-disaster planning strategy to improve access to critical services. This paper introduces an optimization-based approach to locate and configure electric power-generating resilience hubs considering the possibility of failures in transportation and electric power systems. The model's objective is to identify hub locations and configurations that maximize transportation accessibility to the hubs and maximize the satisfaction of basic energy needs through hub-generated electric power. Besides a budget constraint, the model accounts for limits on the levels of hub energy generation vis-à-vis community energy demands, and on the transportation network distance of communities to hubs. Three heuristics are presented for the proposed planning problem. The first heuristic is a genetic algorithm (GA) with problem-specific solution generation procedures. The other two heuristics implement greedy search techniques. Numerical experiments were conducted, using data from rural Puerto Rico, to illustrate the application of the proposed model and heuristics, and examine their performance. In the numerical experiments, the GA heuristic found better solutions than the greedy heuristics. Additionally, design solutions consisting of spatially dispersed hubs with low energy generation capacity were better than solutions with spatially concentrated high-capacity hubs. Lastly, across a wide range of hub demand scenarios, only a small number of candidate hub locations consistently ranked among the best locations for establishing a hub.

1. Introduction

Power outages and roadway failures are common events after major natural disasters. A dramatic example of these disruptions occurred after Hurricane María struck Puerto Rico in 2017, which damaged or destroyed dozens of roadways and bridges, and caused one of the longest blackouts in history (Colucci Ríos, 2018; Kwasinski et al., 2019). Among the responses to this crisis was the establishment of solar energy-based hubs by non-profit groups. These hubs provided to the most vulnerable members of society the opportunity to charge their electronic devices, power medical devices, and receive other types of services (Mignoni, 2018). Energy hubs are an example of the emerging concept of a resilience hub, that is, a community-based physical space designed to provide services and supplies before, during, or after a disaster (Ciriaco and Wong, 2022). Besides providing community support in connection with major disasters, the decentralized energy generated by resilience hubs could provide aid during smaller scale events that nonetheless prove fatal to vulnerable community members, such as the blackouts that accompany extreme heat wave events (Stone et al., 2022). Energy resilience hubs could additionally facilitate communities' transition to clean energy mobility alternatives, such as integrated solar power-based energy-mobility hubs.

The effectiveness of a resilience hub depends, in part, on its location and transportation accessibility. In their review of the resilience hub

* Corresponding author.
E-mail addresses: daniel.rodriguez6@upr.edu (D. Rodriguez-Roman), hector.carlo@upr.edu (H.J. Carlo), joshua.sperling@nrel.gov (J. Sperling), andrew.duvall@nrel.gov (A. Duvall), ruben.leoncio@upr.edu (R.E. Leoncio-Cabán), carla.lopezdelpuerto@upr.edu (C. López del Puerto).

https://doi.org/10.1016/j.trip.2024.101079
Received 15 November 2023; Received in revised form 15 February 2024; Accepted 23 March 2024

concept and associated transportation needs, Ciriaco and Wong (2022) found a lack of research on methods to optimize the placement of these centers. Fortunately, a considerable number of models have been developed to optimize the position of facilities, supplies, and other assets as part of pre-disaster planning (Sabbaghtorkan et al., 2020). The primary objective of this paper is to extend the facility location optimization problem to address the problem of locating and configuring energy resilience hubs considering transportation and electric power system failures and community needs.

Like in previous facility location models, the proposed optimization model accounts for uncertainty in transportation link availability and service demand levels prior to a disaster, but it additionally considers the uncertainty in the damage to the electric power distribution links and the spatial and temporal extent of power outages. Besides optimizing hub locations, the model considers energy system configuration decisions for each hub. The model is formulated as a bi-objective, nonlinear integer optimization problem. The two objectives considered are: maximizing the expected community access to the hub energy services and maximizing the satisfaction of energy needs. Constraints on the level of hub energy generation and on the distance of communities to hubs are also considered. Lastly, the paper presents three heuristics for the proposed problem.

Including the introduction, this paper is composed of six sections. The next section reviews literature on pre-disaster facility location problems. The third and fourth sections present the model formulation and proposed heuristics, respectively. The application of the proposed methods is illustrated using the case of Puerto Rico. Concluding remarks and future research opportunities are presented in the last section.

2. Literature review

Major disasters have motivated an extensive body of work on facility location problems for emergency humanitarian logistics (FLPEs) in the context of multiple types of events, such as hurricanes, earthquakes, and flooding. The models have been developed to guide decisions at the pre-disaster, disaster, and post-disaster stages (Kara and Sava, 2017), and they have been applied to determine the optimal location of distribution centers, shelters, warehouses, storage facilities, rescue helicopters, ambulances, and medical facilities, among other types of facilities. FLPEs generally seek a set of facility locations that: i) minimize the sum of a humanitarian cost metric, including the economic cost of human suffering (Holguín-Veras et al., 2013); ii) cover the users demand within distance or time limits (set covering problems); iii) minimize the maximum distance of any demand location to a facility (minimax problems); iv) account for the impact of decisions made across time (dynamic problems) and/or v) incorporate uncertainty into the optimization process (e.g., stochastic and robust optimization problems) (Boonmee et al., 2017). FLPEs that account for uncertainty in pre-disaster planning are discussed next. For a more expansive review of FLPEs and related humanitarian logistic literature, see (Boonmee et al., 2017; Liberatore et al., 2013).

For pre-disaster planning, the exact location and magnitude of a natural disaster is uncertain, which means that the origin and scale of the demand for facility services, the state of the transportation network connecting the demand points to the facilities, and the condition of the facilities after the disaster are also uncertain (Liberatore et al., 2013). For this reason, researchers have introduced uncertainty to the formulations of pre-disaster FLPEs. For example, Ukkusuri and Yushimito (2008) developed a location-routing problem for emergency inventory prepositioning that considers the probability that routes connecting facilities fail; the failure probabilities are assumed to be independent and known. Balcik and Beamon (2008) account for demand uncertainty in the development of a set covering problem that can be used to determine the location of distribution centers and their inventory levels. Using a set of discrete demand scenarios, their modeling approach seeks to maximize the expected benefits to potentially affected individuals. Rawls and Turnquist (2010) proposed a two-stage stochastic mixed integer program for the pre-positioning of emergency storage facilities that considers uncertainty in demand levels and transportation link availability, also using a set of discrete scenarios that represent uncertain disaster events. Besides the locations, the model accounts for the sizes of storage facilities, the quantity of materials stored in each facility, and the distribution of supplies. The possibility of facility failures has also been considered, as in the model proposed by Galindo and Batta (2013). To account for demand uncertainty, Galindo and Batta specify probability distributions for the demand at each demand point, and they introduce a constraint to ensure that supply levels at each demand point meets the expected demand times a safety factor. Shu et al. (2023) also account for demand uncertainty using probability distributions that are used as part of a chance-constrained stochastic programming model.

Besides minimizing total costs or maximizing benefits, the fair allocation of resources is a basic consideration in humanitarian logistics and FLPEs. For instance, using the concept of conditional value-at-risk, Chapman and Mitchell (2018) developed a FLPE model that minimizes cost disparities among members of the population. Erbeyoğlu and Bilge (2020) proposed a FLPE that considers fairness goals through service coverage windows constraints that ensure demand satisfaction levels. Equity and fairness considerations are often integrated as part of multi-objective FLPEs, as in the work of Mohammadi et al. (2016), who presented a stochastic programming model for supply prepositioning that considers the objectives of maximizing total expected demand coverage, minimizing total expected cost, and minimizing the difference in the satisfaction rates between demand points. For additional details regarding pre-disaster FLEPs under uncertainty, see (Sabbaghtorkan et al., 2020).

The optimal location, size, and mix of components of electric power generation, distribution, and transmission systems is also a well-established research field, with works that consider the deployment of small-scale energy systems given natural hazards (Nourollahi et al., 2021; Rezaee Jordehi, 2016). However, to the authors' knowledge, this is the first paper to consider the problem of optimizing location and scale of facilities to satisfy basic energy needs in the event of a natural disaster from a humanitarian logistics perspective. Similar to previous work, uncertainty in the availability of transportation network components is considered, but the proposed model also considers the uncertainty in electric power services given a disaster.

3. Model formulation

The notation used for the model formulation is presented in Table 1. The facility location optimization model is developed based on the following assumptions:

- A1: A decision-maker (e.g., a government agency) is interested in determining the optimal set of hub locations and configurations with the goal of improving community resilience to power outages caused by disasters.
- A2: There is a hub implementation budget B that constraints the number of hubs that can be established, as well as their energy generations capacity.
- A3: A set of discrete scenarios $s \in \boldsymbol{S}$ representing different disasters (e.g., type, location, magnitude) and associated states of the transportation and electric power systems is available, and each scenario s has a probability of occurrence ρ^s.
- A4: Behavioral models are available that can be used to compute the probability that members of a community would use a particular hub.
- A5: A hub must have the capacity to satisfy the basic energy needs of all the communities that are closest to it.

The key result of the optimization model is the selection of locations to establish hubs and their energy generation capacity. Let $\boldsymbol{J}$ be a given

Table 1
Notation.

Type	Symbol	Definition
Index	i	Index for community locations (zones)
	j, a	Indices for hub locations
	r	Index for hub configuration types
	s	Index for disaster scenarios
	g	Index of population groups
Set	$\boldsymbol{G}$	Population groups in the service region
	$\boldsymbol{I}$	Community locations
	$\boldsymbol{J}$	Candidate hub locations ($j \in \boldsymbol{J}$)
	$\boldsymbol{S}$	Disaster scenarios
	$\boldsymbol{R}_j$	Energy system configurations at each hub location $j \in J$
	$\boldsymbol{T}^s$	Transportation and electric power network graphs under scenario s
	$\boldsymbol{T}$	Set of all $\boldsymbol{T}^s$
	$\boldsymbol{X}$	Decision variables
	$\boldsymbol{\vartheta}_g$	Sociodemographic characteristics of group g
	Θ_j^s	Set of communities whose closest hub is j in scenario s
Decision Variable	x_{jr}	1 if a hub of type r is established in location j, and 0 otherwise
Parameter	B	Budget
	c_{jr}	Cost of establishing a type r hub in location j
	d_{max}	Maximum desirable distance between a community and its closest hub
	d_{ij}^s	Shortest path distance between zone i and location j in scenario s
	h_{gi}	Daily basic electric power needs of group (g,i)
	κ	Threshold probability for $\Psi_i(\boldsymbol{T},\boldsymbol{X},d_{max})$
	μ	Threshold probability for $\Gamma_j(\boldsymbol{T},\boldsymbol{X},\Lambda)$
	η_{gi}	Number of members in group (g,i)
	ρ^s	Probability of occurrence of disaster scenario s
	t_i^s	Number of days without electricity at location i in the disaster scenario s
	ω_A, ω_Z	Objective function weights
	γ_j^s	Energy generation efficiency factor for hub j in scenario s
	m_r	Energy generation capacity of hub configuration r
Function	$\Lambda(\boldsymbol{T},\boldsymbol{X},\boldsymbol{G})$	Patterns in hub choice and energy consumption behaviors
	$A(\boldsymbol{T},\boldsymbol{X},\Lambda)$	Measure of community access to the hub
	$Z(\boldsymbol{T},\boldsymbol{X},\Lambda)$	Measure of energy need satisfaction
	$\Psi_i(\boldsymbol{T},\boldsymbol{X},d_{max})$	Probability that a community i is within a distance d_{max} from its closest hub is greater
	$\Gamma_j(\boldsymbol{T},\boldsymbol{X},\Lambda)$	Probability that an energy hub can generate the energy required by communities closest to it
	$V_{gijr}^s(\boldsymbol{T}^s,\boldsymbol{X},\boldsymbol{\vartheta}_g)$	Utility that group g in zone i derives from the energy services at hub j under scenario s; V_{gi-}^s is the utility of not using a hub
	u_{gi}^s	Probability that group g in zone i chooses to use a hub
	$W_i^s(\boldsymbol{X},\boldsymbol{T}^s,d_{max})$	Indicator:1 if zone i is within d_{max} distance from a hub in scenario s
	E_j^s	Energy generation of hub j in scenario s
	L_j^s	Energy demand that hub j must satisfy under scenario s
	Q_j^s	Indicator:1 if $L_j^s \le E_j^s$; 0 otherwise

set of candidate hub locations, $\boldsymbol{R}_j$ be the set of possible energy system configurations available at each hub location $j \in J$, and x_{jr} be a binary decision variable that equals 1 if a hub of type $r \in \boldsymbol{R}_j$ is established in location j, and 0 otherwise. $\boldsymbol{X}$ is the set of all variables x_{jr}. Also, define c_{jr} as the cost of establishing a type r hub in location j. The set $\boldsymbol{I}$ denotes the community nodes (zones) of interest.

Let $\boldsymbol{T}^s$ represent the transportation and electric power network graphs under scenario s and let the set of these graphs be $\boldsymbol{T}$ ($\boldsymbol{T}^s \in \boldsymbol{T}$). The decision-maker's objectives depend on the patterns $\Lambda(\boldsymbol{T},\boldsymbol{X},\boldsymbol{G})$ in hub choice and energy consumption behaviors that arise given the energy hubs locations and configurations indicated in $\boldsymbol{X}$, the spatial and sociodemographic characteristics of the population groups in the service region, represented by set $\boldsymbol{G}$, and the transportation and electric transmission networks $\boldsymbol{T}$ (for notational simplicity, the arguments of Λ will be omitted hereafter). The decision-maker's objectives are to maximize a measure of community access $A(\boldsymbol{T},\boldsymbol{X},\Lambda)$ to the hubs and to maximize a measure of energy need satisfaction $Z(\boldsymbol{T},\boldsymbol{X},\Lambda)$, subject to a set of constraints. Related to this objectives, the model includes constraints that ensure that the probability $\Psi_i(\boldsymbol{T},\boldsymbol{X},d_{max})$ that a community i is within a distance d_{max} from its closest hub is greater or equal than κ (Equation (4), and that the probability $\Gamma_j(\boldsymbol{T},\boldsymbol{X},\Lambda)$ that an energy hub can generate the energy required by communities closest to it is equal to or greater than μ (Equation (5). With the given notation and assumptions, the decision-maker's optimization problem can be generally stated as:

$$\max F = \{A(\boldsymbol{T},\boldsymbol{X},\Lambda), Z(\boldsymbol{T},\boldsymbol{X},\Lambda)\} \tag{1}$$

subject to

$$\sum_{j\in\boldsymbol{J}}\sum_{r\in\boldsymbol{R}_j} c_{jr}x_{jr} \le B \tag{2}$$

$$\sum_{r\in\boldsymbol{R}_j} x_{jr} \le 1, \forall j \in \boldsymbol{J} \tag{3}$$

$$\Psi_i(\boldsymbol{T},\boldsymbol{X},d_{max}) \ge \kappa, \forall i \in \boldsymbol{I} \tag{4}$$

$$\Gamma_j(\boldsymbol{T},\boldsymbol{X},\Lambda) \ge \mu\sum_{r\in\boldsymbol{R}_j} x_{jr}, \forall j \in \boldsymbol{J} \tag{5}$$

$$x_{jr} = \{0,1\}, \forall j \in \boldsymbol{J}, r \in \boldsymbol{R}_j \tag{6}$$

Equations (2) is the budget constraint and Equation (3) ensures that at most one type of hub design is selected for each location. Equations (4) and (5) ensure, to a degree, that a community is within a maximum distance from a hub and that energy hubs can generate the energy required by communities closest to it, respectively. Equation (6) forces the variables to be binary. The following subsections propose specific formulations for the objective functions and Equations (4) and (5). The process of disaster scenario generation, including the determination of each scenario's probability of occurrence, depends on the type of disaster under consideration (e.g., storms, earthquakes, floods), the historical disaster data available, the physical characteristics of the study region (e.g., topography), and available computational models, among other factors. As previously stated, the proposed model assumes as given a set of disaster scenarios and their probability. For a discussion of methods for disaster scenario generation, see, for example, the work of Nowell et al. (1996) and Garn et al. (2023).

3.1. Hub accessibility and energy need objectives

The accessibility to and demand for the energy services of the resilience hubs depends on the status of the transportation and energy networks after a disaster and the energy needs of individuals in the service region. The latter depends, naturally, on the characteristics of the individuals. For example, after a disaster, members of low-income households without power generators are considerably more likely to need and use an energy resilience hub than members of high-income households that own electric power generators. The hub choice behavior of community groups will be modeled using utility and discrete choice theory.

Define $V_{gijr}^s(\boldsymbol{T}^s,\boldsymbol{X},\boldsymbol{\vartheta}_g)$ as the utility that group $g \in \boldsymbol{G}$ in zone i derives from the energy services at hub j under scenario s given the network state under scenario s ($\boldsymbol{T}^s$) and sociodemographic variables $\boldsymbol{\vartheta}_g$ (e.g., income). The utility function V_{gijr}^s can capture the effects that, for example, the distance, travel time, service wait times, and sociodemographic attributes have on a group's hub choice behavior. For example, V_{gijr}^s can be formulated as the following linear-in-parameters utility function:

$$V_{gijr}^s = \beta_0 + \beta_d d_{ij}^s + \beta_g z_g + \beta_r z_r \tag{7}$$

where $\beta_0, \beta_d, \beta_g$ and β_r are estimated model parameters, d_{ij}^s is the shortest path distance between node pair ij for scenario s, z_g can represent a sociodemographic characteristic such as average group income, and z_r can be dummy variable that indicates the utility derived by users given hub configuration r. The β parameters can be estimated using discrete choice analysis based on observed hub choice behavior after a disaster (i.e., revealed preference data) or stated hub choice behavior obtained through community surveys prior to a disaster event (i.e., stated prefence data) (Ben-Akiva and Lerman, 1985).

If it is assumed that the choice probabilities are modeled using the commonly applied multinomial logit (MNL) model, the accessibility of a group to the hub services can be defined as the expected utility of the available choice set (also known as the logsum) (Ben-Akiva and Lerman, 1985; de Jong et al., 2007), which results in the following expression (omitting utility arguments and assuming that the logit scaling parameter is set to one):

$$A_{gi}^s = \ln\left(e^{V_{gi-}^s} + \sum_{j\in \boldsymbol{J}}\sum_{r\in \boldsymbol{R}_j} x_{jr} e^{V_{gijr}^s}\right) \tag{8}$$

The V_{gi-}^s term in Equation (8) refers to the utility of not using a hub. Equation (8) offers theoretically sound scalar summary of the expected worth that the available choices have for a group given that group's sociodemographic characteristics $\boldsymbol{\vartheta}_g$ and the status of the networks $\boldsymbol{T}^s$. It is also a standard approach to measure accessibility in the transportation planning context. Using Equation (8) and defining η_{gi} as the number of members in group (g,i), the measure of the community access $A(\boldsymbol{T},\boldsymbol{X},\Lambda)$ can defined as the expected accessibility measure:

$$A(\boldsymbol{T},\boldsymbol{X},\Lambda) = \sum_{s\in \boldsymbol{S}} \rho^s \sum_{i\in \boldsymbol{I}}\sum_{g\in \boldsymbol{G}} \eta_{gi} A_{gi}^s \tag{9}$$

In this expression the hub service demand patterns Λ is captured by the discrete choice models via the V_{gijr}^s terms, which depend on $\boldsymbol{T}$ and $\boldsymbol{X}$. The term η_{gi} could be eliminated from Equation (9) if the analyst was more interested achieving equitable access across groups, regardless of their population size.

The measure of energy need satisfaction $Z(\boldsymbol{T},\boldsymbol{X},\Lambda)$ can also be formulated using the outputs of discrete choice models. Let h_{gi} represent the daily basic electric power needs of group (g,i) (e.g., charging electronic devices, powering medical devices (IEA, 2020)), u_{gi}^s be the probability that the group chooses to use a hub (given by the choice models), and t_i^s denote the number of days without electric power service at location i in the disaster scenario s. Then, $Z(\boldsymbol{T},\boldsymbol{X},\Lambda)$ can be defined as the expected consumption of the hub-generated electric power

$$Z(\boldsymbol{T},\boldsymbol{X},\Lambda) = \sum_{s\in \boldsymbol{S}} \rho^s \sum_{i\in \boldsymbol{I}} t_i^s \sum_{g\in \boldsymbol{G}} \eta_{gi} h_{gi} u_{gi}^s \tag{10}$$

Under the MNL model assumption, the probability of using a hub can be computed using:

$$u_{gi}^s = 1 - \frac{e^{V_{gi-}^s}}{e^{V_{gi-}^s} + \sum_{j\in \boldsymbol{J}}\sum_{r\in \boldsymbol{R}_j} x_{jr} e^{V_{gijr}^s}} \tag{11}$$

This probability increases as the hubs are closer and more convenient for a group. Note that the formulations for the objective functions are positive correlated via the V_{gijr}^s: as the hub utility functions increase, so do the accessibility measure, the probability of using a hub, and the hub energy consumption. In general, like in these formulations, one would expect that the objective of maximizing accessibility to the resilience hubs is not necessarily in conflict with the objective of maximizing the use of the hub-generated electric power, as increasing transportation accessibility would increase the probability that people use the hubs. Given the objectives complementarity, a useful approach to solve the bi-objective problem in Equation (1) is to convert it into a single objective optimization problem using linear scalarization, which results in:

$$F = \omega_A A(\boldsymbol{T},\boldsymbol{X},\Lambda) + \omega_Z Z(\boldsymbol{T},\boldsymbol{X},\Lambda) \tag{12}$$

where ω_A and ω_Z are objective weights set by the analyst to combine the objectives. The values ω_A and ω_Z could be set, for example, so that the objective is in monetary units (e.g., using the concept of marginal utility of income for the accessibility term (de Jong et al., 2007) and willingness-to-pay analysis for the energy term). Alternatively, the weights could be set to represent the importance that the decision maker gives to each objective. In the case study, the weights are set so that the value of both objectives have similar magnitudes.

3.2. Ensuring a minimum level of hub spatial proximity

The purpose of the constraints in Equation (4) is to ensure a minimum level of spatial proximity for every community, up to a threshold set by the decision-maker. Equation (4) can be operationalized using the set of discrete scenarios $\boldsymbol{S}$. Each disaster scenario s results in a distinct transportation network that produces different shortest path distances from each community $i \in \boldsymbol{I}$ to each candidate location $j \in \boldsymbol{J}$. These shortest path distances can be determined prior to the analysis (i.e., they are model parameters). Given a hub location and configuration solution $\boldsymbol{X}$, the only relevant shortest path distances are those of candidate locations for which hubs have been selected, that is, j locations for which $\sum_{r\in \boldsymbol{R}_j} x_{jr} = 1$. Let d_{ij}^s be the shortest past distance between zone i and hub location j in scenario s and define the indicator:

$$W_i^s(\boldsymbol{X},\boldsymbol{T}^s,d_{max}) = \begin{cases} 1 & if \min_{\forall j\in \boldsymbol{J}}\left(d_{ij}^s + d_{max}\left(1 - \sum_{r\in \boldsymbol{R}_j} x_{jr}\right)\right) \le d_{max} \\ 0 & otherwise \end{cases} \tag{13}$$

Then, probability $\Psi_i(\boldsymbol{T},\boldsymbol{X},d_{max})$ that a community i is within a distance d_{max} from its closest hub can be stated as:

$$\Psi_{id}(\boldsymbol{T},\boldsymbol{X},d_{max}) = \sum_{s\in \boldsymbol{S}} \rho^s W_i^s(\boldsymbol{X},\boldsymbol{T}^s,d_{max}) \tag{14}$$

3.3. Modeling hub energy generation and consumption to ensure minimum service levels

Equation (5) ensures that the daily level of electric power generation at the hubs is such that basic electric power needs of the communities are satisfied to a degree specified by the decision-maker. Let m_r represent the energy generation capacity of hub configuration r under ideal conditions and γ_j^s be an efficiency factor that reflects conditions that affect the location's energy generation capacity $(0 < \gamma_j^s \le 1)$. For example, if the hubs generate electricity using solar-based systems, γ_j^s could reflect the meteorological conditions in scenario s that affect the hub's energy generation output. Given this notation, the energy generation of the hub E_j^s under scenario s is:

$$E_j^s = \gamma_j^s \sum_{r\in \boldsymbol{R}_j} x_{jr} m_r \tag{15}$$

E_j^s should satisfy the energy needs of the groups that travel to j. As an energy safety policy, here it is assumed that a hub should have the capacity to satisfy the basic energy needs of all the communities that are closest to it. Define Θ_j^s as the set of communities whose closest hub is j in scenario s (i.e., $\Theta_j^s = \left\{i \in \boldsymbol{I} : j = \underset{a\in \boldsymbol{J}}{\operatorname{argmin}}(d_{ia})\right\}$). With the given assumptions, the energy demand that the hub at j must satisfy in scenario s is:

$$L_j^s = \sum_{r\in \boldsymbol{R}_j} x_{jr} \sum_{i\in \Theta_j^s}\sum_{g\in \boldsymbol{G}} \eta_{gi} h_{gi} u_{gi}^s \tag{16}$$

An alternative to Equation (16) and the underlying assumptions is to build a model based on the assumption that a deterministic or stochastic energy demand equilibrium, or some other demand distribution mechanism, can be formulated to estimate the distribution of community members across the hub locations that surround them. However, after a disaster, where communities have incomplete and changing information, and urgent needs, it is unlikely that a type of energy demand equilibrium is reached in the middle of the emergency, and it is arguably more reasonable to make planning decisions under the simpler assumption that people will travel to their closest available hub.

The probability $\Gamma_j(\boldsymbol{T}, \boldsymbol{X}, \Lambda)$ that a hub will satisfy the potential energy loads given the different disaster scenarios can be computed using an indicator variable. Define the indicator:

$$Q_j^s\left(L_j^s, E_j^s\right) = \begin{cases} 1 & if L_j^s \le E_j^s \\ 0 & otherwise \end{cases} \tag{17}$$

Then $\Gamma_j(\boldsymbol{T}, \boldsymbol{X}, \Lambda)$ can be formulated as:

$$\Gamma_j(\boldsymbol{T}, \boldsymbol{X}, \Lambda) = \sum_{s \in \boldsymbol{S}} \rho^s Q_j^s\left(L_j^s, E_j^s\right) \tag{18}$$

4. Heuristics

Three heuristics are proposed for the hub location problem. The first heuristic is based on the genetic algorithm, a solution approach used in previous FLPE studies (Boonmee et al., 2017). The other two heuristics implement greedy search strategies that take advantage of the problem constraints.

4.1. Genetic algorithm

Genetic algorithms (GAs) offer a flexible, derivative-free approach to search for optimization problem solutions (Deb, 1999). GAs are evolution-inspired procedures that interactively improve upon a set of candidate solutions, which in GA terminology are individually called chromosomes and collectively called the population. In the proposed approach, a solution chromosome n is represented by the vector $\boldsymbol{x}_n$ of length equal to the number of candidate hub locations ($|\boldsymbol{J}|$). Let x_{jn} be an element of $\boldsymbol{x}_n$ whose integer value represents the hub type implemented at location j. x_{jn} equal to zero indicates that no hub is located at j, while integer values greater than zero are the index of the hub type implement at j. Problem-specific search strategies were introduced within the general GA framework to improve its exploratory efficiency and accelerate the discovery of good $\boldsymbol{x}_n$ designs.

A high-level description of the main components of the proposed GA is presented next. Detailed descriptions of the main steps are offered in the next subsections. The general steps of the proposed GA are:

Step 0:	*Initialization.* Initial parameter values required by the GA steps are set.
Step 1:	*Generate an initial population.* Apply procedures to generate an initial set of candidate solutions to the design problem. In Section 4.1.1, two new problem-specific mechanisms are proposed to generate an initial set of feasible candidate solutions. The mechanisms consider the budget constraint and the general objective of selecting hub locations that are close to the community zones.
Step 2:	*Evaluate the fitness of candidate solutions.* For each unexamined chromosome in the population, determine the chromosome's fitness based on its objective function and constraints values. Section 4.1.2 explains the expression used to compute a chromosome's fitness.
Step 3:	If the maximum number of candidate chromosomes has been evaluated, return the best solution in the population, and stop the iterative process. Otherwise, continue to Step 4.
Step 4:	*Select parent population:* Based on the fitness evaluation, apply a procedure to select the set of chromosomes to combine and mutate in order to create a new generation of solutions (offspring). The standard tournament selection method was used in the numerical experiments discussed in Section 5 to select the parent population (Deb, 1999).

(*continued on next column*)

(*continued*)

Step 5.	*Generate offspring solutions.* Apply crossover and mutation operations to generate new candidate solutions by combining and changing the information contained in the parent population. In Section 4.1.3, a new crossover operation procedure is proposed that considers the spatial characteristics of a candidate solution
Step 6.	Pool the offspring and parent chromosomes to create a new population and return to Step 2.

4.1.1. Procedure to generate initial population

The initial population of solutions is generated using two strategies. Both depend on the number of hubs that can be reasonably installed given the budget constraint and the implementation costs of each hub type. The lower (y_{lb}) and upper (y_{ub}) bounds on the number of hubs that can be implemented in a region can be computed using the expressions $y_{lb} = \lfloor B/c_{max} \rfloor$ and $y_{ub} = \lfloor B/c_{min} \rfloor$, where c_{min} and c_{max} are minimum and maximum cost of the hub types under consideration. Given these bounds, the first chromosome generation strategy randomly selects locations among the candidate locations $\boldsymbol{J}$, while the second strategy randomly selects hub locations that are closest to the zones $\boldsymbol{I}$, as indicated by the distance matrix $\boldsymbol{D}$ (dimensions $|\boldsymbol{I}| \times |\boldsymbol{J}|$). $\boldsymbol{D}$ contains the average shortest distance, across all scenarios, between the zones and the candidate hub locations. The first strategy is executed with probability ρ_{rand} and the second strategy is executed with probability $1 - \rho_{rand}$, until N_0 chromosomes are generated. The initial population procedure (IIP) and its strategies consists of the following steps.

Step 0:	Set $n = 1$, compute the distance matrix $\boldsymbol{D}$, and create the empty set $\boldsymbol{X}$.
Step 1:	Set $\boldsymbol{x}_n$ as a zero vector with dimensions $1 \times |\boldsymbol{J}|$ and create the empty set Y_n.
Step 2:	Generate the total number of hubs y to locate for chromosome n by taking a random integer draw from the interval $[y_{lb}, y_{ub}]$.
Step 3:	Draw w from the standard uniform distribution.
Step 4:	If $w < \rho_{rand}$:
Step 5:	(Apply Strategy 1) For k ranging from 1 to y:
Step 6:	Randomly select a hub location index j not in Y_n, and store it in Y_n.
	Else:
Step 7:	(Apply Strategy 2) For k ranging from 1 to y:
Step 8:	If $\boldsymbol{D}$ is not empty:
Step 9:	For each candidate hub location, use $\boldsymbol{D}$ to compute the average shortest path distance to all zones in $\boldsymbol{I}$.
Step 10:	From the b hub locations with lowest average distance to the zones, randomly select a hub location index j not in Y_n, and store it in Y_n.
Step 11:	Update $\boldsymbol{D}$ by removing the column corresponding to the previously selected location, and the rows for all zones within d_{max} of the selected location.
	Else:
Step 12:	Randomly select a hub location index j not in Y_n, and store it in Y_n.
Step 13:	For each selected hub location in Y_n, determine the least expensive hub configuration that satisfies the energy constraints (Equation (5) and store the configuration type in $\boldsymbol{x}_n$; if no hub type satisfies a constraint, select the hub type with the maximum energy capacity.
Step 14:	Store $\boldsymbol{x}_n$ in $\boldsymbol{X}$.
Step 15:	If $n > N_0$, stop; otherwise, set $n = n + 1$ and return to Step 1.
Step 16:	Return $\boldsymbol{X}$.

Note that in Step 13, for each selected hub location j, the Θ_j^s set of communities for which j is their closest hub must be identified, and their aggregate demand must be computed to evaluate Equation (5).

4.1.2. Fitness evaluation and parent selection

In GA terminology, the fitness value of a chromosome measures how good a solution it is. Here, the fitness value is determined by computing the objective function (Equation (12) and the constraints. If a chromosome is feasible, its fitness is the value of Equation (12); otherwise, its fitness is computed using the penalty method (Deb, 2000). For an

infeasible chromosome n, let ξ_{nB} be 1 if the budget constraint is not satisfied, and zero otherwise; let be ξ_{nd} represent the number of zones i for which Equation (4) is not satisfied; and let ξ_{nd} be the number of selected hub locations for which Equation (5) is not satisfied. Also, define F_{min} as the lowest objective function value among the feasible solutions, if there are no feasible solutions set $F_{min} = 0$. Then, the fitness of infeasible solution n is computed using:

$$F_n = F_{min} - p_B\xi_{nB} - p_d\xi_{nd} - p_e\xi_{ne} \tag{19}$$

where p_B, p_d, and p_e are penalty factors for each type of constraint. Given the fitness values of each chromosome, a parent population (most promising chromosomes) of size N was selected in each iteration using tournament selection (Deb, 1999).

4.1.3. Crossover and mutation operations

Crossover and mutation operators were used to generate offspring chromosomes (new candidate solutions) based on the parent population. First, the operators produce vectors x'_n of length equal to $1 \times |J|$. The values of the vector elements indicate the selected hub locations: $x'_{nj} = 1$ if location j has a hub, and $x'_{nj} = 0$ otherwise. Given x'_n, the hub type vector x_n is produced using the same procedure as in Step 13 of the IIP.

Two strategies were implemented for the crossover operation. With probability ρ_{cross}, a single-point crossover operation (Deb, 1999) was performed to generate x'_n and, with probability $1 - \rho_{oc}$, a spatial crossover operation was performed. As illustrated in Fig. 1, the spatial crossover operation considers the spatial distribution of the candidate hub locations. The geographic space that contains the candidate hub locations is divided into two regions using a randomly generated line and, based on these regions, the hub location information is swapped between parents to create a new x'_n vector.

The mutation operator is applied at the vector element level. With probability ρ_{mut}, a hub is added to location j if $x'_{nj} = 0$ or, if there is a hub at j, it is moved to another randomly selected location that does not have a hub. The algorithm for generating an offspring population of size $2 \times N$ is presented next:

Step 0:	Read parent population X, and create the empty sets X_{cross} and X_{mut}.
Step 1:	(Apply Crossover Operation) For k ranging from 1 to N:
Step 2:	Set x_k as a zero vector with dimensions $1 \times \|J\|$

(continued on next column)

(continued)

Step 3:	Draw two parent chromosomes from X and find their vectors x'^1_n and x'^2_n.
Step 4:	Draw w from the standard uniform distribution.
Step 5:	If $w < \rho_{cross}$:
Step 6:	Use the single-point crossover to generate offspring x'_k based on x'^1_n and x'^2_n.
	Else:
Step 7:	Use the spatial crossover to generate offspring x'_k based on x'^1_n and x'^2_n.
Step 8:	For each selected hub location in x'_k, determine the least expensive hub configuration that satisfies Equation (5) and store the configuration type in x_k; if no hub type satisfies a constraint, select the hub type with the maximum energy capacity.
Step 9:	Store x_k in X_{cross}.
Step 10:	(Apply Mutation Operation) For k ranging from 1 to N:
Step 11:	Set $\chi = 0$ and randomly draw a solution from $X \cup X_{cross}$; call its location vector x'_k.
Step 12:	For j ranging from 1 to $\|J\|$:
Step 13:	Draw w from the standard uniform distribution.
Step 14:	If $w < \rho_{mut}$:
Step 15:	Set $x'_{kj} = 1$ if $x'_{kj} = 0$; otherwise, set $x'_{kj} = 0$ and randomly select a location to add a hub. Set $\chi = 1$.
Step 16:	If $\chi = = 1$, repeat the procedure described in Step 8, and store the resulting x_k in X_{mut}.
Step 17:	Return X_{cross} and X_{mut}.

In this algorithm, the combined population $X \cup X_{cross} \cup X_{mut}$ is evaluated using the fitness function and using their fitness values a new parent population X is selected using tournament selection. The GA search process continues until the number of evaluated solutions is greater than a given number. To avoid repeated solutions, chromosomes in $X_{cross} \cup X_{mut}$ that have been previously evaluated can be eliminated.

4.2. Greedy Reduction heuristic

The proposed FLPE seeks to maximize an objective function that is limited by only one "less than or equal to" restriction, the budget constraint. The Greedy Reduction Heuristic (GRH) is designed to take advance of this tradeoff. Without loss of generality, it is assumed that the

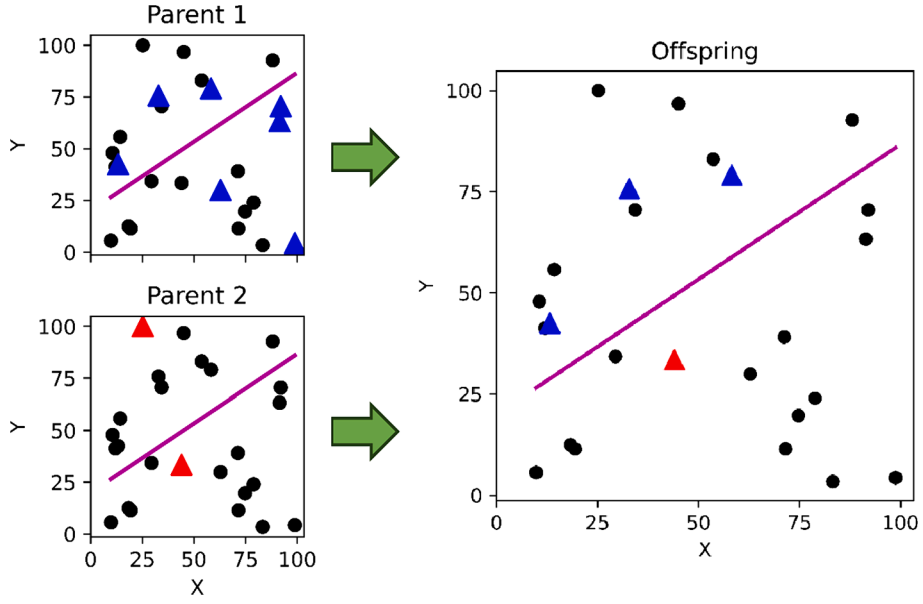

Fig. 1. Spatial crossover operation (dots: candidate hub locations; triangles: selected locations).

cost of a configuration is directly proportional to the amount of energy that it produces. GRH will start with the most expensive configuration and will progressively reduce the configuration for one hub until the budget constraint is met. GRH can be summarized as follows:

Step 1:	Start with the most expensive configuration in each candidate hub location. This configuration will be feasible for all restrictions, except for the budget restriction.
Step 2:	Evaluate reducing one level of configuration for each candidate hub location and select the one that: (a) maintains feasibility of Equation (4) and Equation (5), and (b) has the least impact on the objective function value.
Step 3:	If Equation (2) is feasible, go to Step 4; otherwise, return to Step 2.
Step 4:	Return best solution.

4.3. Greedy increase heuristic

The Greedy Increase Heuristic (GIH) takes a complementary approach to GRH. GIH starts with no active hubs and progressively adds configuration levels to the system until all constraints are met. GIH is said to be complementary to GRH as the budget constraint is maintained feasible and the system cost is increased until the other restrictions are met. GIH can be summarized as follows:

Step 1:	Start with no active hubs. This configuration will only be feasible for the budget restriction.
Step 2:	Evaluate adding one level of configuration for each candidate hub location and select the one that: (a) maintains feasibility of Equation (2), and (b) has the greatest impact on the objective function value.
Step 3:	If Equation (4) and Equation (5) are feasible, go to Step 4; otherwise, return to Step 2.
Step 4:	Return best solution.

5. Numerical experiments

Numerical experiments were conducted using data from the remote central rural region of Puerto Rico (PR). The goal of the numerical experiments was to illustrate the application of the model and examine the performance of the heuristics. Budget levels, logit model parameters, and algorithm parameters were varied in tests to explore the sensitivity of key model metrics. The data files and scripts that contain the models and parameters used in the experiments can be found in an online repository (Rodriguez-Roman, 2023).

5.1. Model parameters

In Fig. 2, the zonal system and the road network for the region are presented. The region's 272 US Census block groups were used as the zonal system. Population and income data from the US Census were obtained for each zone. The region has a population of 126,767 people, which were divided into three income groups: low income (income less than $30,000), medium income (income between $30,000 and $74,999), and high income (income greater than or equal to $75,000). The low-income, mid-income, and high-income groups represent 72 %, 24 %, and 4 % of the population. In total, there were 816 distinct groups differianted by zone and income. Each individual in these groups was assumed to have the same basic electric power demand of 5 W-hour. The groups' utility functions were defined as follows:

$$V^s_{gi-} = \beta_0 + \beta_{LI} z_{gLI} + \beta_{MI} z_{gMI} + \beta_{HI} z_{gHI} \quad (20)$$

$$V^s_{gij} = -0.06 \times d^s_{ij}/805 \quad (21)$$

where z_{gLI}, z_{gMI}, and z_{gHI} are dummy variables that indicate if g is a low-, mid-, or high-income group, respectively, and d^s_{ij} is the shortest path distance between pair ij for scenario s. The 805 value is an average speed in meters/minute unit, which is used to convert the distance to travel time. The −0.06 parameter was borrowed from a logit model estimated using stated-preference data from a survey conducted in PR after the 2022 passage of Hurricane Fiona (the survey that explored the potential demand for resilience hubs). The values of the remaining utility function parameters ($\beta_0, \beta_{LI}, \beta_{MI}, \beta_{HI}$) were assumed for the purposes of the numerical experiments. Table 2 reports the utility function parameter values; note that at least one of the income group dummy parameters must be set to zero, and therefore $\beta_{HI} = 0$ in all tests. The characteristics of the hub configurations used in the experiments are presented in Table 3.

The road network is composed of 1124 nodes and 391 links (not counting zone centroid connectors). A total of 113 locations were identified as candidate hub sites. Ten scenarios were generated by simulating hurricane trajectories over PR. For each scenario, the likelihood of road link failures and the duration of power outages for each zone were simulated as a function of the perpendicular distance of roads and zones to the hurricane trajectory. Note that link failures affect the shortest path distances between zones and hub locations. In addition, it was assumed that the hub configurations used solar-based systems to generate energy, and for each scenario s and location j an efficiency factor γ^s_j was generated using solar geospatial data for PR obtained from the National Renewable Energy Laboratory. Each scenario was assigned

Table 2
$\boldsymbol{\beta}$ Parameters.

Set ID	β_0	β_{LI}	β_{MI}	β_{HI}
$\boldsymbol{\beta}$-Set 1	2	0.1	0.05	0
$\boldsymbol{\beta}$-Set 2	1.75	0	0	0
$\boldsymbol{\beta}$-Set 3	1.5	0	0	0
$\boldsymbol{\beta}$-Set 4	1.25	−0.10	−0.05	0
$\boldsymbol{\beta}$-Set 5	1	−0.10	−0.05	0

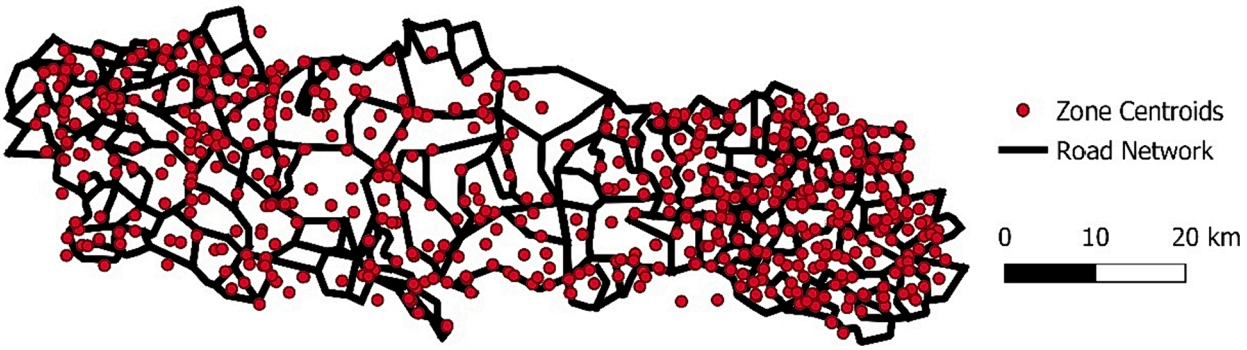

Fig. 2. Zone centroids and road network (centroid connectors omitted).

Table 3
Characteristics of the hub configurations.

Type	Energy Generation Capacity (watt-hour)	Cost ($)
1	25,000	200,000
2	50,000	225,000
3	75,000	350,000
4	100,000	450,000
5	150,000	500,000

the same probability of occurring. The parameters ω_1, ω_2, d_{max}, κ, and μ were set to the values of 1, 0.1, 16 km, 0.8, and 0.8, respectively.

5.2. Trials and results

Three sets of trial tests were performed to explore: 1) the performance of the proposed heuristics, 2) the impact of different budget levels, and 3) the impact of higher and varied hub demand patterns. In the first set of trials the three heuristics were applied to find solutions to the PR hub location and configuration problem. The first application test assumed a budget of $2 million and the $\boldsymbol{\beta}$-Set 1 parameters. The performance of the GA heuristic was examined using different algorithmic parameters. In particular, the test examined the impact on GA performance of ρ_{rand} and ρ_{cross}. ρ_{rand} controls the type of strategy used to generate the initial set of solutions in each GA run, while ρ_{cross} controls the type of crossover operation applied. The six sets of combinations of ρ_{rand} and ρ_{cross} values used in the test are reported in Table 4. For each set of GA parameters, 50 runs of the GA were performed until 100,000 solutions were evaluated. Multiple runs were performed as the GA is a stochastic search algorithm and several outcomes would be needed to compute meaningful performance statistics, and 100,000 solutions were evaluated in each run as experience suggests that each GA run would have converged to after that number of chromosome evaluations. In each run, parameters N, $N_0(2 \times N)$, and ρ_{mut} were set to 64, 128, 0.05, respectively, as typically population sizes of around 20 to 200 individual solutions produce good results and mutation rates are commonly set to low values around 0.01 (e.g., Li and Yeh, 2005). The parameters p_B, p_d, and p_e were all are set to 1 to give equal penalty to each type of constraint, and the parameters y_{lb}, y_{ub} and b were given the values of 5, 12, and 5, respectively, given the $2 million budget and the assumed minimum and maximum cost of the hubs presented in Table 3,

Table 4 reports performance statistics for the runs of each GA parameter set, along with the results obtained for the GRH and GIH. Fig. 3 shows the progression of the median value of the maximum objective function value found in the GA trials. GRH found its best solution after 57,462 solution evaluations, while GIH found its solution after 114 evaluations. The greedy heuristics have no parameters, and their output is deterministic. Based on the results reported in Table 4 and

Table 4
GA parameters and results for numerical experiments.

Heuristic	Best objective function (F) Value			Coefficient of Variation
	Mean	Minimum	Maximum	
GA - Set 1: $\{\rho_{rand} = 0, \rho_{cross} = 0\}$	659,059	649,144	698,870	0.028
GA - Set 2:$\{\rho_{rand} = 0, \rho_{cross} = 0.5\}$	663,645	649,144	696,685	0.028
GA - Set 3:$\{\rho_{rand} = 0, \rho_{cross} = 1\}$	659,059	649,144	696,685	0.026
GA - Set 4:$\{\rho_{rand} = 0.5, \rho_{cross} = 0\}$	654,922	630,368	692,280	0.020
GA - Set 5:$\{\rho_{rand} = 0.5, \rho_{cross} = 0.5\}$	652,181	637,211	696,685	0.025
GA - Set 6:$\{\rho_{rand} = 0.5, \rho_{cross} = 1\}$	651,452	635,765	697,671	0.027
GRH	630,368			–
GIH	322,528			–

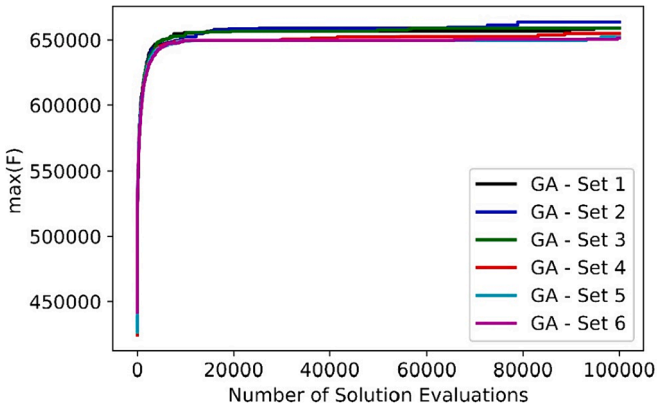

Fig. 3. Median value of the maximum objective function value in the GA trials.

Fig. 3, the GA heuristic outperformed the greedy heuristics. On average, the best performing GA instance had parameter Set 2: $\{\rho_{rand} = 0, \rho_{cross} = 0.5\}$. This GA instance produced solutions with an objective function value 5.3 % higher than the best performing greedy heuristic (GRH). When $\rho_{rand} = 0$, only Strategy 2 of the IIP is used. This suggests that it is useful to start the search for solutions by establishing hubs in locations that are closest to the population zones, which makes intuitive sense. When $\rho_{cross} = 0.5$, on average, half of the crossover operations apply the single-point method, and the other half apply the spatial crossover approach, suggesting that the new crossover operator developed for this problem is useful, but only in conjunction with more standard crossover techniques.

In the second set of trials experiments were conducted to explore the impact of budget increases on the values of the objective function (F), the accessibility to the hubs (A), the expected satisfaction of energy needs (Z), and the distribution of the hubs. Budget increases of 125 %, 250 %, 375 % and 500 %, relative to $2 million, were used in these tests. The best GA-generated results obtained with the different budgets were compared relative to the best GA-generated solution obtained using a budget of $2 million (GA-Set 2 used in all runs). In Fig. 4, the percentage changes in the values of F, A, and Z functions are reported. As expected, as the budget increases, the function values increase, although not at the same rate. A 500 % budget increase ($10 million) resulted in an increment of 80 % in F, with the Z objective exhibiting more improvement relative to the A objective. A greater budget means that more hubs can be implemented, as shown in Fig. 5. Interestingly, in these series of tests the cheapest hub was selected in all solutions, which maximizes the number of hubs and their spatial distribution, given the budget constraint. Activating more hubs reduces the groups' shortest path distance to its closest hub, as shown in Fig. 6. The budget experiments were

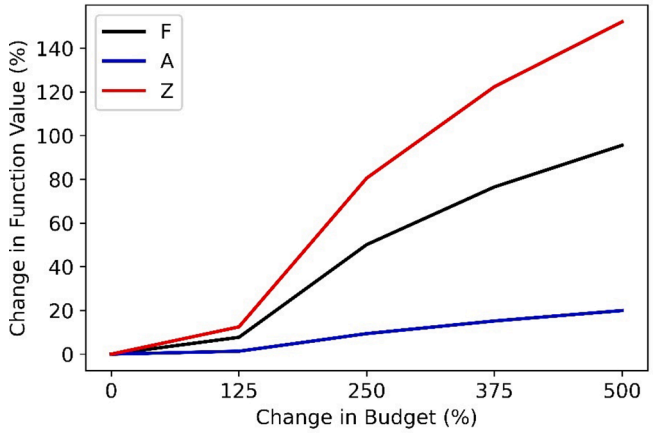

Fig. 4. Percentage change in objective functions given the budget increments.

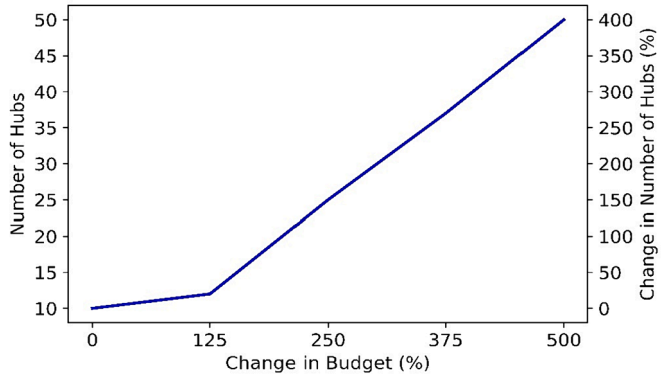

Fig. 5. Change in number of hubs given the budget increments.

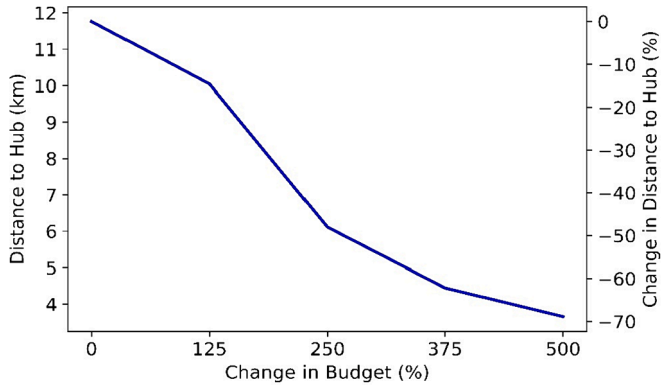

Fig. 6. Shortest path distance to a hub given the budget increments.

also conducted with the greedy heuristics, and, as before, the GA also outperformed them, with the lowest difference in best objective function values being of 8.6 %.

The last set of trials explored the impact of higher and varied hub demand patterns, particularly in terms of the energy consumption and generation profiles. Higher demand levels were achieved using the utility function parameters (the $\boldsymbol{\beta}$-sets) presented in Table 2. In these trial runs, the budget was set to $2,000,000. Each of the $\boldsymbol{\beta}$-set results presented next was obtained using the best design solution $\boldsymbol{X}$ generated by the GA-Set 2 heuristic, with 5 runs per $\boldsymbol{\beta}$ set. As Fig. 7 illustrates, the higher the $\boldsymbol{\beta}$-set ID, the higher the probability that the population in a community would use a hub, and, therefore, the higher the hub demand levels. The maximum ratio – across the disaster scenarios – of the total hub energy consumption and the total hub energy generation is presented in Fig. 8. Interestingly, despite the increasing hub demand levels produced by each successive $\boldsymbol{\beta}$ set, the ratio hovers around 8 % (i.e., only 8 % of the generated energy is consumed). The higher demand levels force a shift from 10 hub locations in the best design solution obtained for β-Set 1 to nine hub locations in the remaining $\boldsymbol{\beta}$ sets, all with higher presence of Type 2 hub configurations and higher maximum energy generation capacity, as shown in Fig. 9. Higher demand levels also made it harder for the GA to generate feasible solutions that satisfied the energy constraints, as illustrated in Fig. 10, which presents the percentage of generated designs that were feasible (i.e., feasibility rate) in the runs for each $\boldsymbol{\beta}$ set.

The $\boldsymbol{\beta}$ sets in Table 2 successively increase the demand for hub energy services in a spatially uniform manner, as the utility parameters do not vary by zone. To explore the impact of spatially varied demand levels on the stability of the selected hub locations, 100 GA trial runs were performed in which each zone was assigned a different β_0 parameter value and all income group parameters were set to 0. Each one of the 100 GA runs represents a different hub demand scenario. In each GA run and for each zone i, the value of the β_{0i} parameter was determined by taking a random draw from a normal distribution with mean 1 and standard deviation 0.5. The outputs of the 100 GA runs were analyzed to determine the percentage that each candidate hub location was selected to establish a hub as part of a run's best design solution; Figs. 11 and 12 present the results of the analysis. As Fig. 11(a) and Fig. 12 show, a limited number of candidate locations were selected to establish a hub in the trial runs. Of the 113 possible candidate hub locations, 41 % were not selected in any of the 100 demand scenario runs, whereas around 25 % of candidate locations were selected in 12 % or more of the runs. Four candidate hub locations, which constitute only 3.5 % of all candidate locations, were selected to establish a hub in 50 % or more trial runs, as indicated by the red spots in the contour map presented in Fig. 11(a). For reference, in Fig. 12(b) a contour map of the population concentration is presented.

5.3. Discussion

As expected, increasing budget levels increase the optimal number of established hubs, but there are diminishing returns to this investment, as can be seen in Fig. 4. The numerical experiments showed that the best performing design solutions had spatially dispersed resilience hubs with low power generating capacity, as opposed to solutions with spatially concentrated, high-capacity hubs. In part, this result can be explained by the accessibility objective function as its value increases when communities' distance to hubs decreases, and a greater number of spatially dispersed hubs reduces these distances. Given the budget constraint, the spatially dispersed hubs must have the least costly and feasible energy generating capacity. Additionally, the results presented in Figs. 11 and 12 suggest that there is a limited set of candidate locations that are

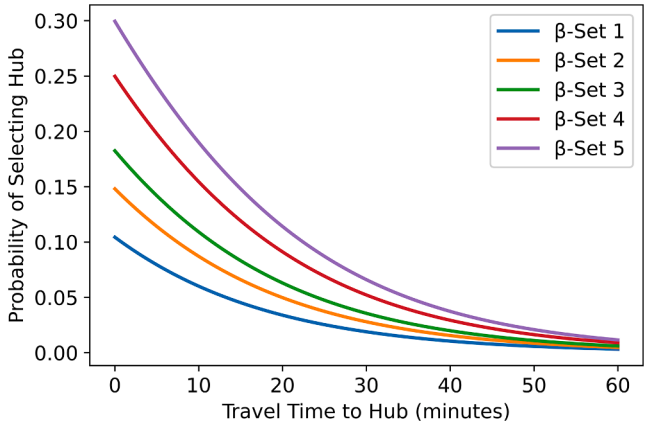

Fig. 7. Probability of selecting a hub for low-income group.

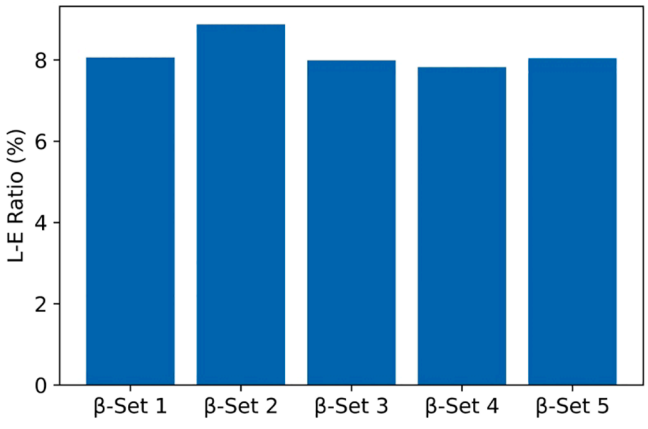

Fig. 8. Maximum ratio of energy demanded ($\boldsymbol{L}$) and energy generated..($\boldsymbol{E}$)

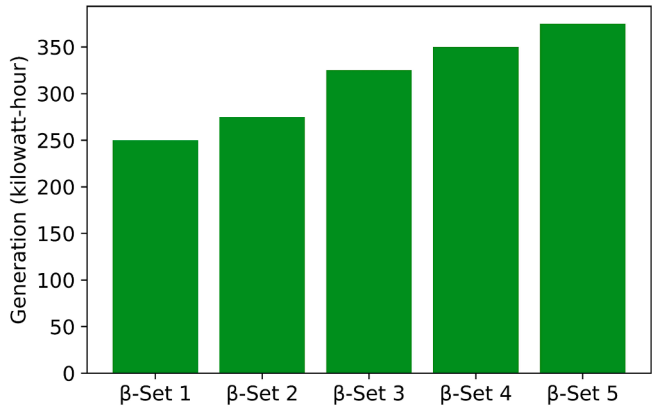

Fig. 9. Maximum energy generated by the best hub arrangement for each β set.

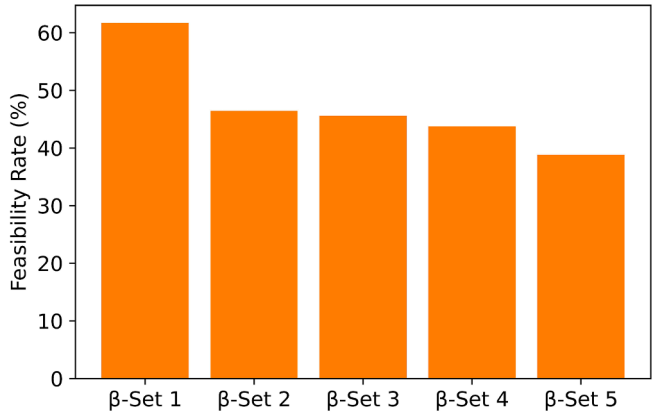

Fig. 10. GA solution feasibility for each β set.

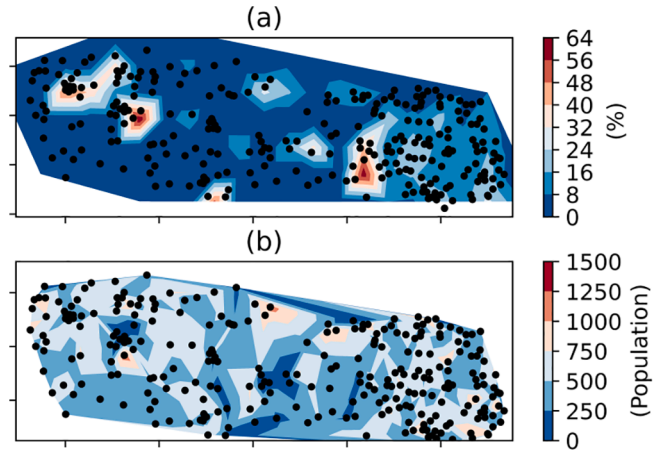

Fig. 11. Maps of (a) hub location selection percentage and (b) population concentration (black dots are the zone centroids).

particularly promising across a wide range of demand scenarios. In the experiments, only 3.5 % of the considered candidate hub locations were part of design solutions in more than 50 % of the demand scenarios. In practice, the sensitivity analysis performed here could be used to identify the best set of hub locations, particularly when there is considerable uncertainty regarding hub demand levels or the interest of communities in resilience hubs.

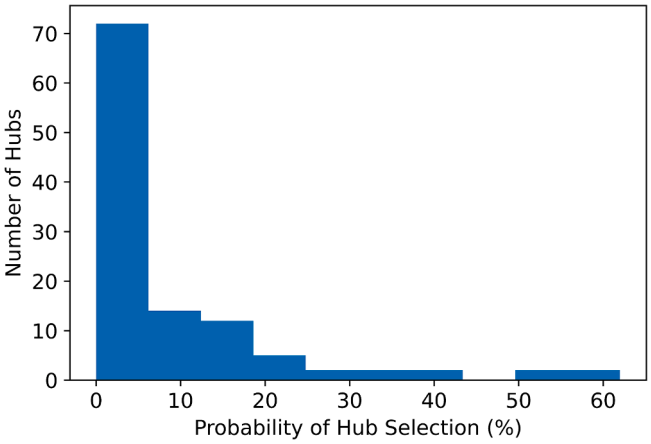

Fig. 12. Frequency of hub selection percentage.

6. Closing remarks

A facility location problem for the optimal placement and configuration of energy resilience hubs was presented, along with three heuristics. The model considers the objectives of maximizing transportation accessibility to the hubs and maximizing satisfaction of basic energy needs, subject to constraints on the implementation cost, distance between communities and their closest hub, and energy generation levels at the hubs. The GA had the best performance of the three heuristics developed for the planning problem. The experiments showed that, for the model system considered, there is decreasing marginal benefits, in terms of the objective function value components (F, A, Z), as the hub implementation budget is increased.

The main limitation of the proposed methodology is its reliance on discrete choice models to estimate the potential community demand levels for resilience hubs. In practice, planners are unlikely to have access to models of hub choice behavior that could be used to simulate people's interest in and potential use of resilience hubs. To overcome this limitation, community outreach is needed to: 1) determine the factors that people consider important when deciding whether to use a resilience hub after a disaster and 2) gather data on people's stated hub choice behavior given hypothetical disaster scenarios. Using these data, discrete choice models could be estimated to model people's preferences for resilience hubs. Alternatively, planners could assume reasonable values for the logit model parameters, perhaps borrowed from the discrete choice models in regional travel forecasting models, and conduct sensitivity analyses such as those performed in this paper to select candidate hub locations and capacities. Another model limitation is that only basic energy needs are considered. The complexities introduced by the need to charge electric vehicles after a disaster were not considered in this paper. Future research could explore what additional hub features, beyond energy generation capacity, should be incorporated to the model to account for electric vehicle charging needs.

Future research should consider strategies to linearize the proposed problem (e.g., the decision variables could be continuous if hub energy capacity is stated as a linear function of the monetary investment on a hub location). Future research can also explore how mobility services can be optimally integrated in disaster resilience hubs. For example, the hubs can be a center for shared light electric vehicles (e.g., e-bikes) offering mobility solutions to individuals who find themselves without their private vehicles in the aftermath of a disaster. Another potential research subject is the impact of queuing delays at resilience hubs and their impact on the benefits that individuals obtain from their services. In terms of heuristic development, further research could be completed that implements more graph-based search techniques to identify optimal hub location; the proposed GA only used graph-based search in Strategy 2 of the IPP.

CRediT authorship contribution statement

Daniel Rodriguez-Roman: Conceptualization, Formal analysis, Funding acquisition, Investigation, Methodology, Project administration, Software, Visualization, Writing – original draft, Writing – review & editing. **Hector J. Carlo:** Conceptualization, Formal analysis, Investigation, Methodology, Writing – original draft. **Joshua Sperling:** Conceptualization, Writing – original draft. **Andrew Duvall:** Conceptualization, Writing – original draft. **Rubén E. Leoncio-Cabán:** Formal analysis, Software. **Carla López del Puerto:** Conceptualization, Funding acquisition, Writing – original draft.

Declaration of competing interest

The authors declare the following financial interests/personal relationships which may be considered as potential competing interests: Daniel Rodriguez-Roman reports financial support was provided by National Science Foundation. If there are other authors, they declare that they have no known competing financial interests or personal relationships that could have appeared to influence the work reported in this paper.

Data availability

The data and programs that support the findings of this study are openly available in OSF at https://osf.io/sw8k2/.

Acknowledgments

This work was supported by the National Science Foundation under Grants No. 1832468, 1832427 (HSI program) and 2228601. Any opinions, findings, and conclusions or recommendations expressed in this material are those of the authors and do not necessarily reflect the views of the National Science Foundation.

The authors thank the Comité Comunal of Corcovada for sharing their perspectives on community resilience to natural disasters, and Dr. Stanley Young for his helpful suggestions.

References

Balcik, B., Beamon, B.M., 2008. Facility location in humanitarian relief. Int. J. Log Res. Appl. 11, 101–121. https://doi.org/10.1080/13675560701561789.

Ben-Akiva, M., Lerman, S.R., 1985. Discrete Choice Analysis. MIT Press, Cambridge, MA.

Boonmee, C., Arimura, M., Asada, T., 2017. Facility location optimization model for emergency humanitarian logistics. Int. J. Disaster Risk Reduct. 24, 485–498. https://doi.org/10.1016/j.ijdrr.2017.01.017.

Chapman, A.G., Mitchell, J.E., 2018. A fair division approach to humanitarian logistics inspired by conditional value-at-risk. Ann. Operat. Res. 262, 133–151. https://doi.org/10.1007/s10479-016-2322-1.

Ciriaco, T.G.M., Wong, S.D., 2022. Review of resilience hubs and associated transportation needs. Transp. Res. Interdiscip. Perspect. 16, 100697 https://doi.org/10.1016/j.trip.2022.100697.

Colucci Ríos, B., 2018. Lessons learned on the passage of category 5 hurricane Maria over the island of Puerto Rico: road safety infrastructure perspective. 18th International Conference Road Safety on Five Continents.

de Jong, G., Daly, A., Pieters, M., van der Hoorn, T., 2007. The logsum as an evaluation measure: review of the literature and new results. Transp. Res. Part A Policy Pract. 41, 874–889. https://doi.org/10.1016/j.tra.2006.10.002.

Deb, K., 1999. An introduction to genetic algorithms. Sadhana 24, 293–315. https://doi.org/10.7551/mitpress/3927.001.0001.

Deb, K., 2000. An efficient constraint handling method for genetic algorithms. Comput. Methods Appl. Mech. Eng. 186, 311–338. https://doi.org/10.1177/0305829815620047.

Erbeyoğlu, G., Bilge, Ü., 2020. A robust disaster preparedness model for effective and fair disaster response. Eur J Oper Res 280, 479–494. https://doi.org/10.1016/j.ejor.2019.07.029.

Galindo, G., Batta, R., 2013. Prepositioning of supplies in preparation for a hurricane under potential destruction of prepositioned supplies. Socioecon Plann Sci 47, 20–37. https://doi.org/10.1016/j.seps.2012.11.002.

Garn, B., Kieseberg, K., Schreiber, D., Simos, D.E., 2023. Combinatorial sequences for disaster scenario generation. Operat. Re. Forum 4. https://doi.org/10.1007/s43069-023-00225-4.

Holguín-Veras, J., Pérez, N., Jaller, M., Van Wassenhove, L.N., Aros-Vera, F., 2013. On the appropriate objective function for post-disaster humanitarian logistics models. J. Oper. Manag. 31, 262–280. https://doi.org/10.1016/j.jom.2013.06.002.

IEA, 2020. Defining energy access: 2020 methodology [WWW Document]. URL https://www.iea.org/articles/defining-energy-access-2020-methodology.

Kara, B.Y., Sava, S., 2017. Humanitarian logistics. In: INFORMS Tutorials in Operations Research, pp. 272–309. https://doi.org/10.1287/educ.2017.0174.

Kwasinski, A., Andrade, F., Castro-Sitiriche, M.J., O'Neill-Carrillo, E., 2019. Hurricane Maria effects on Puerto Rico electric power infrastructure. IEEE Power Energy Technol. Syst. J. 6, 85–94. https://doi.org/10.1109/jpets.2019.2900293.

Li, X., Yeh, A.G.O., 2005. Integration of genetic algorithms and GIS for optimal location search. Int. J. Geogr. Inf. Sci. 19, 581–601. https://doi.org/10.1080/13658810500032388.

Liberatore, F., Pizarro, C., de Blas, C.S., Ortuño, M.T., Vitoriano, B., 2013. Uncertainty in humanitarian logistics for disaster management. A Review 45–74. https://doi.org/10.2991/978-94-91216-74-9_3.

Mignoni, E., 2018. Puerto Rico's solar-powered energy oasis [WWW Document]. accessed 6.26.23 Yale Climate Connections. https://yaleclimateconnections.org/2018/04/puerto-ricos-solar-powered-energy-oasis/.

Mohammadi, R., Ghomi, S.M.T.F., Jolai, F., 2016. Prepositioning emergency earthquake response supplies: a new multi-objective particle swarm optimization algorithm. Appl Math Model 40, 5183–5199.

Nourollahi, R., Salyani, P., Zare, K., Mohammadi-Ivatloo, B., 2021. Resiliency-oriented optimal scheduling of microgrids in the presence of demand response programs using a hybrid stochastic-robust optimization approach. Int. J. Electr. Power Energy Syst. 128, 106723 https://doi.org/10.1016/j.ijepes.2020.106723.

Nowell, H.K., Horner, M.W., Widener, M.J., 1996. Impacts of disrupted road networks in siting relief facility locations: case study for Leon County. Florida. https://doi.org/10.1061/(ASCE)NH.1527-6996.0000168.

Rawls, C.G., Turnquist, M.A., 2010. Pre-positioning of emergency supplies for disaster response. Transp. Res. B Methodol. 44, 521–534. https://doi.org/10.1016/j.trb.2009.08.003.

Rezaee Jordehi, A., 2016. Allocation of distributed generation units in electric power systems: a review. Renew. Sustain. Energy Rev. 56, 893–905. https://doi.org/10.1016/j.rser.2015.11.086.

Rodriguez-Roman, D., 2023. Repository for Resilience Hub Project [WWW Document]. URL https://osf.io/sw8k2/.

Sabbaghtorkan, M., Batta, R., He, Q., 2020. Prepositioning of assets and supplies in disaster operations management: review and research gap identification. Eur. J. Oper. Res. 284, 1–19. https://doi.org/10.1016/j.ejor.2019.06.029.

Shu, J., Song, M., Wang, B., Yang, J., Zhu, S., 2023. Humanitarian relief network design: responsiveness maximization and a case study of typhoon Rammasun. IISE Trans 55, 301–313. https://doi.org/10.1080/24725854.2022.2074577.

Stone, B., Gronlund, C.J., Mallen, E., Hondula, D., O'Neill, M.S., Rajput, M., Grijalva, S., Lanza, K., Harlan, S., Larsen, L., Augenbroe, G., Krayenhoff, E.S., Broadbent, A., Georgescu, M., 2022. How blackouts during heat waves amplify mortality and morbidity risk. Environ Sci Technol. https://doi.org/10.1021/acs.est.2c09588.

Ukkusuri, S.V., Yushimito, W.F., 2008. Location routing approach for the humanitarian prepositioning problem. Transp. Res. Rec. 18–25 https://doi.org/10.3141/2089-03.